Development of Steering Control System for Autonomous Vehicle Using Geometry-Based Path Tracking Algorithm

Myungwook Park, Sangwoo Lee, and Wooyong Han

In this paper, a steering control system for the path tracking of autonomous vehicles is described. The steering control system consists of a path tracker and primitive driver. The path tracker generates the desired steering angle by using the look-ahead distance, vehicle heading, and a lateral offset. A method for applying an autonomous vehicle to path tracking is an advanced pure pursuit method that can reduce cutting corners, which is a weakness of the pure pursuit method. The steering controller controls the steering actuator to follow the desired steering angle. A servo motor is installed to control the steering handle, and it can transmit the steering force using a belt and pulley. We designed a steering controller that is applied to a proportional integral differential controller. However, because of a dead band, the path tracking performance and stability of autonomous vehicles are reduced. To overcome the dead band, a dead band compensator was developed. As a result of the compensator, the path tracking performance and stability are improved.

Keywords: Autonomous vehicle, steering control system, geometry path-tracking method.

I. Introduction

With advancements in information and communication and vehicle techniques, the competition to develop and commercialize intelligent and autonomous vehicles has intensified. The aim of these vehicles is to secure vehicle stability and driver ease, as well as to enhance traffic efficiency.

The intelligent Advanced Driver Assistance System (ADAS) helps drivers through a human–machine interface by following the lane departure warning system, Lane Keeping Assistance System (LKAS), Forward Collision Warning System, and Smart Parking Assistant System (SPAS). LKAS helps a car stay on course near the center of a lane by continuously applying a small amount of counter-steering force when the system senses the vehicle deviating from its lane [1]. SPAS helps make parking easier by providing automatic steering assistance along a preset path to guide a driver to the optimal position from which to start backing into a parking space [2]. An autonomous vehicle is a vehicle that can drive itself to a destination without its driver having to recognize the driving environment. This paper describes the method of path tracking and the development of a steering control system using techniques applied to intelligent and autonomous vehicles.

The geometric path-racking method is one of the most popular methods, following pure pursuit, vector pursuit, and the Stanley method. The pure pursuit method is relatively easy to implement and is robust to large disturbances. However, this method has a problem of cutting corners at high speed, because the look-ahead distance increases along with an increase in vehicle speed. In addition, steady-state errors occur at high

speed. The Stanley method has a better tracking performance than the pure pursuit method under most driving environments. In addition, because it uses the lateral offset from the front axle of the vehicle to the path, the Stanley method does not incur the problem of cutting corners but does incur an overshooting of turns. It is also influenced by various disturbances [3]. The vector pursuit method uses the theory of screws. The vector pursuit method is similar to a pure pursuit method. However, this method is less sensitive regarding the look-ahead distance than the pure pursuit method [4]. The pure pursuit method is used to apply path tracking to an autonomous vehicle, is easy to implement, and is robust to large disturbances. In addition, we propose an algorithm to reduce the problem of cutting corners that occurs in the pure pursuit method by using a lateral offset from the rear axle of the vehicle to the path.

To follow a desired steering angle generated by the path tracking algorithm, we have to control the steering handle. Today, the steering system found in most vehicles is that of the motor-driven power steering (MDPS) system. The MDPS system reduces a driver's effort by providing assist torque and return torque based on an electric motor. Recently, the MDPS system has been applied to the ADAS and autonomous systems, and beyond its original functions, stands in for a driver [5]. However, for security reasons, we cannot control the MDPS system. Therefore, to control the steering handle, we installed an actuator on the steering column. In addition, a proportional integral differential (PID) controller and dead band compensator are applied to control the actuator, and we verified the controller through a field test.

The remainder of this paper is outlined as follows. Section II describes our hardware systems. Section III introduces an overview of the steering control system. The advanced pure pursuit algorithm is then described in Section IV. Section V then presents a primitive driver to control the steering system. The experimental results are provided in Section VI. Finally, some concluding remarks and areas of future work are given in Section VII.

II. Hardware Systems

1. Autonomous Vehicle

We use a commercial sport utility vehicle for applying the lateral control system. Because this vehicle has a lot of space, it is easy to install the power system, controllers, sensors, and actuators used in the autonomous system.

An autonomous vehicle consists of a power module, perception module, decision-making module, and control module. We used a 24 V/100 Ah battery for the power module, which supplies power to each of the other modules using dc-to-
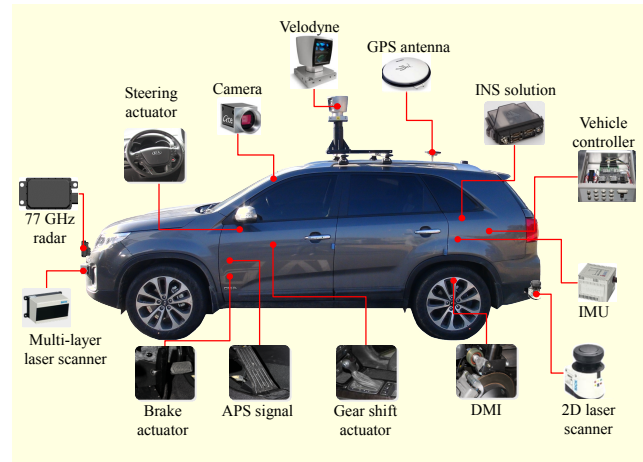

Fig. 1. Hardware system of autonomous vehicle.

dc convertors. In addition, the alternator is installed in the vehicle engine room for charging the battery. The perception module recognizes the driving environment and detects objects and drivable paths using a 2D/3D laser scanner, 77 GHz radar, and a camera. The decision-making module generates the reference path of the vehicle based on the recognition results. The control module controls the vehicle to track the reference path. For path tracking, the steering actuator, brake actuator, and gear shift actuator are equipped in the vehicle. In addition, to know the moving distance and vehicle speed, two distance measurement instruments (DMIs) are implemented in the rear wheels. Because our system is an autonomous system based on the global position of the vehicle, an inertia navigation system (INS) based on a virtual reference station is installed to estimate the vehicle position and dynamics [6]–[7]. The hardware system of the autonomous vehicle is shown in Fig. 1.

2. Steering System

The steering system of most vehicles is an MDPS system. An MDPS system reduces a driver's effort by providing assist torque and return torque using an electric motor. In addition, it is possible to maintain the lane, park automatically, and drive autonomously using the MDPS system. However, for security reasons, we cannot control the MDPS system. Therefore, to track the reference path of the autonomous vehicle, it is possible to control the steering handle by mounting an actuator and reduction gear on the steering column, where the actuator transmits the torque using a belt and pulley. In addition, a potentiometer is equipped to measure the motor position on the motor shaft. These actuators and sensors communicate with the controller using an RS232 and controller area network (CAN). The controller reads the position and speed of the motor from the CAN bus, and it then writes the desired steering PWM signal from the RS232. The hardware system configuration of
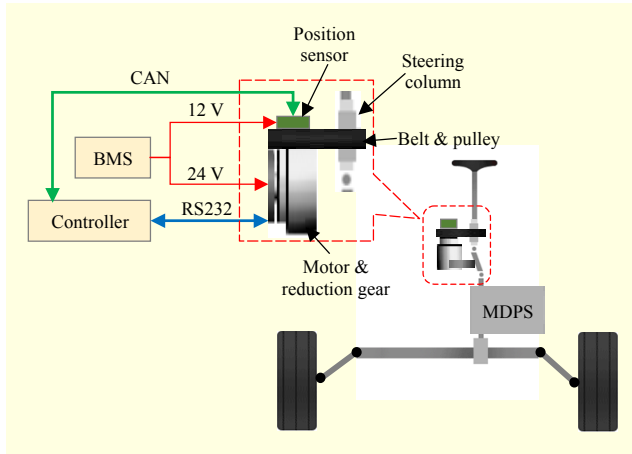
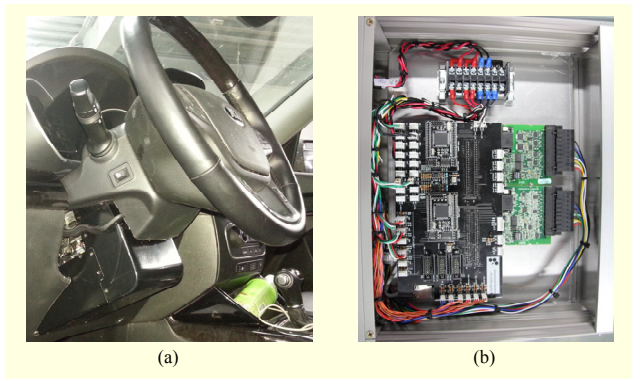Fig. 2. Hardware configuration of steering control system.

Fig. 3. (a) Servo motor and position sensor installed in autonomous vehicle's steering column and (b) steering controller.

the steering control system is shown in Fig. 2, whereas the motor sensor installed in the steering column and the controller are shown in Fig. 3.

III. Steering Control System

The steering control system is a path tracking system that controls the steering actuator based on the current vehicle position, heading from the INS, and reference path from the path planner. The steering control system consists of a path tracker and primitive driver. The path tracker consists of the following three modules: a velocity planning module, look-ahead distance decision module, and path tracking module. The velocity planning module plans the velocity using the curvature of the path, the side friction factor, and the super-elevation. The look-ahead distance decision module determines the look-ahead distance depending on the velocity of the vehicle. In addition, after selecting the goal point on the reference path based on the look-ahead distance, the path tracking module generates the desired steering angle. The primitive driver consists of a throttle/brake controller and
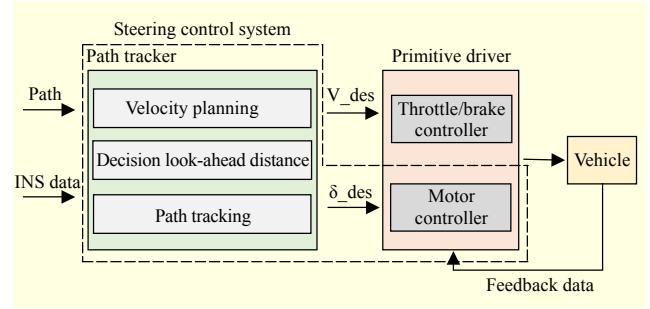

Fig. 4. Block diagram of steering control system.

steering controller. The steering controller controls the steering actuator to follow the reference path. In this paper, we do not deal with a throttle/brake controller. The steering control system is shown by the dotted line in Fig. 4.

IV. Path Tracker

1. Velocity Planning

Velocity planning is needed to prevent slipping and roll-overs when the autonomous vehicle system is running. For this, the velocity planning module plans the velocity using the curvature of the path, the side friction factor, and the super-elevation.

A vehicle driving on a horizontally curved road needs centripetal force for circular motion. Depending on the circular motion, the horizontal curve radius, and speed, the centrifugal force (see Fig. 5) is applied through (1) below. In (1), $\mathbf{g}$ is the gravitational acceleration, $\mathbf{v}$ is the velocity, R is the radius of the curvature, and $\mathbf{w}$ is the weight of the vehicle.

$$\mathbf{f} = \frac{\mathbf{w}}{\mathbf{g}} \times \frac{\mathbf{v}^2}{R}. \tag{1}$$

If the side friction factor is f for the lateral friction force, for vehicle safety, then (2) below is satisfied.

$$(\mathbf{f}\cos\theta - \mathbf{w}\sin\theta) \le f(\mathbf{f}\sin\theta + \mathbf{w}\cos\theta), \tag{2}$$

where θ is the bank angle. Dividing both sides of (2) by $\cos\theta$, we obtain

$$(\mathbf{f} - \mathbf{w}\tan\theta) \le f(\mathbf{f}\tan\theta + \mathbf{w}). \tag{3}$$

Using super-elevation $i = \tan\theta$, substituting (1) into (3), and dividing both sides by $\mathbf{w}$, we obtain the following equation:

$$\left(\frac{\mathbf{v}^2}{\mathbf{g}\cdot R} - i\right) \le f\left(\frac{\mathbf{v}^2}{\mathbf{g}\cdot R}i + 1\right). \tag{4}$$

Assuming $i\cdot f$ is zero in (4), the radius of horizontal curvature is given by
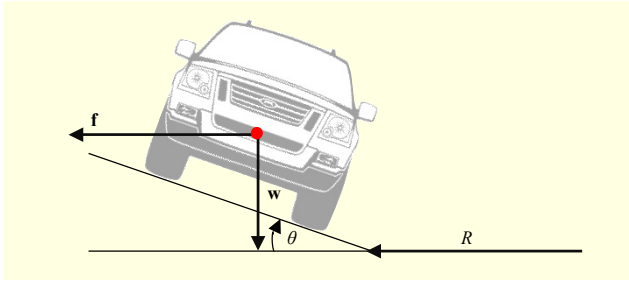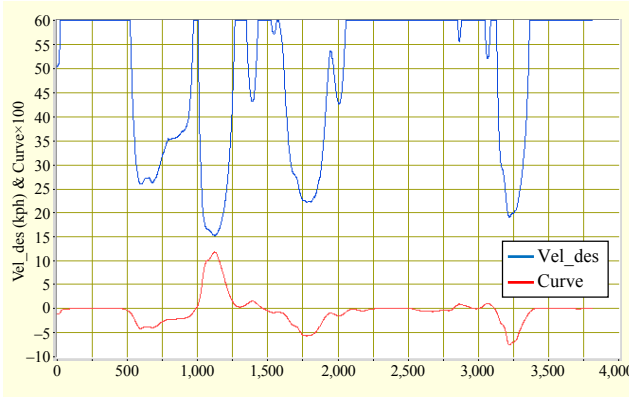
Fig. 5. Acting centrifugal force.

Fig. 6. Desired velocity using curve.

$$R \geq \frac{\mathbf{v}^2}{\mathbf{g}} \cdot \frac{1}{i+f}. \qquad (5)$$

Substituting $1/\kappa$ for R, the limit velocity at a horizontally curved road is calculated through the following equation:

$$\mathbf{v} \leq \sqrt{\frac{\mathbf{g} \cdot (i+f)}{\kappa}}, \qquad (6)$$

where κ is the curvature of the road.

To find the curvature, it is assumed that the path is curved on a plane. In addition, the path is assumed to be approximable by a third-degree polynomial. After approximating a desired path with a third-degree polynomial with curve fitting, the curvatures of the polynomial were determined. From the definition of the curvature, the curvature of the polynomial $y = x(t)$ is shown below.

$$\kappa = \frac{\dfrac{\mathrm{d}^2 y}{\mathrm{d}x^2}}{\left\{ 1 + \left(\dfrac{\mathrm{d}y}{\mathrm{d}x} \right)^2 \right\}^{3/2}}, \qquad (7)$$

The road super-elevation is designed to be 6%–8% when a road is built. In addition, the road super-elevation is limited to below 6% in local and urban roads according to the American Society of State Highway and Transportation Officials publication, *A Policy on Geometric Design of Highways and Streets* [8].

The side friction factor is defined based on the vehicle speed, quality of the road material, and the road conditions (dry, wet, or icy road surface), and is limited to 0.1 to 0.16 depending on the vehicle velocity. The result of the speed according to the curvature is shown in Fig. 6, where the maximum velocity is limited to 60 kph.

2. Determination of Look-Ahead Distance

The magnitude of the look-ahead distance is dynamically adjusted based on the vehicle velocity. A small magnitude of look-ahead distance forces the system to track the path more accurately, and increases in the maximum curvature of a path can be tracked. Additionally, a small look-ahead distance results in oscillation while the vehicle is following the path. Because of this, the vehicle can become unstable. On the other hand, a large magnitude reduces oscillations while tracking the path and allows the vehicle to begin turning before it reaches the curve, resulting in smoother trajectories around sharply curved paths.

In addition, a large magnitude reduces overshoot as the look-ahead distance acts as a damping factor. But if it is too large, then the tracking performance will deteriorate, such as in the cutting corners phenomenon [9].

$$l_\mathrm{d} = \begin{cases} 5 & \mathbf{v}_\mathrm{cur} < 10\,\mathrm{kph}, \\ 0.5 \times \mathbf{v}_\mathrm{cur} & 10\,\mathrm{kph} \leq \mathbf{v}_\mathrm{cur} < 50\,\mathrm{kph}, \\ 25 & 50\,\mathrm{kph} \leq \mathbf{v}_\mathrm{cur}. \end{cases} \qquad (8)$$

S.F. Campbell defined the look-ahead distance as a function of the vehicle velocity and verified that the driving stability of the vehicle increases if the look-ahead distance increases [10]. In this paper, the look-ahead distance is set to between 5 m and 25 m within a velocity range of 10 kph to 50 kph, as shown in Fig. 7.

3. Advanced Path Tracking Algorithm

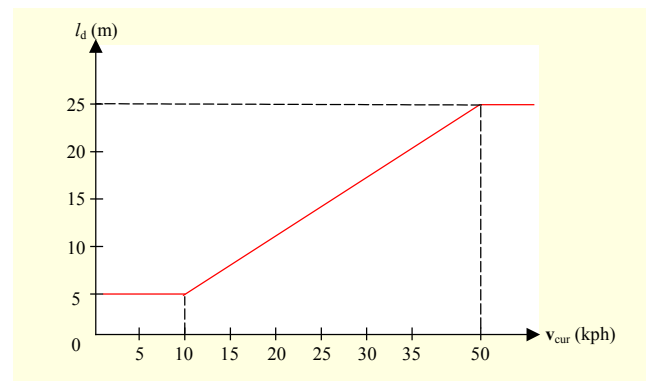The pure pursuit algorithm consists of geometrically

Fig. 7. Look-ahead distance as function of speed.

calculating the curvature of a circular arc that connects the center of the rear axle to the goal point on the path ahead of the vehicle. The goal point is determined from the look-ahead distance (l_{d}). The desired steering wheel angle of the vehicle is determined using angle α between the heading angle of the vehicle and the look-ahead vector. The pure pursuit geometry is shown in Fig. 8.

$$\frac{l_{\mathrm{d}}}{\sin(2\alpha)} = \frac{R}{\sin\left(\frac{\pi}{2} - \alpha\right)}, \tag{9}$$

$$\frac{l_{\mathrm{d}}}{2\sin(\alpha)\cos(\alpha)} = \frac{R}{\cos(\alpha)}, \tag{10}$$

$$\frac{l_{\mathrm{d}}}{\sin(\alpha)} = 2R, \tag{11}$$

$$\kappa = \frac{2\sin(\alpha)}{l_{\mathrm{d}}}, \tag{12}$$

where κ is the curvature of the circular arc. Applying an Ackerman model with two degrees of freedom, the steering angle is given as

$$\delta = \tan^{-1}(\kappa L), \tag{13}$$

where L is the wheel base. Using (12) and (13), the desired steering angle can be written as

$$\delta_{l_{\mathrm{d}}}(t) = \tan^{-1}\left(\frac{2L\sin\big(\alpha(t)\big)}{l_{\mathrm{d}}}\right). \tag{14}$$

The pure pursuit is influenced by the look-ahead distance, which is dynamically adjusted with the velocity. A characteristic of the pure pursuit is that a sufficient look-ahead distance will result in cutting corners while tracking a curved path. To improve this characteristic and steady-state error, we use the lateral offset (error) between the vehicle and path. The examples of lateral offset are shown in Fig. 9. To the left is the cutting corners phenomenon, and to the right is the steady-state error. To reduce the lateral offset, we apply proportional-integral (PI) control theory, as in equation (15) below.

The desired steering angle according to the lateral offset $\delta_{e_{\mathrm{y}}}(t)$ is the sum of the proportional term $\mathcal{P}e_{\mathrm{y}}(t)$ and integral term $\mathcal{Q}(\kappa(t))\int e_{\mathrm{y}}\mathrm{d}t$, where $\mathcal{P}$ and $\mathcal{Q}(\kappa(t))$ are the proportional and integral gains, respectively; both of which are positive values.

The proportional term performs the role of reducing the lateral offset by reducing the target steering in the cutting corners phenomenon. On the other hand, the integral term is useful when a path has a small curvature and eliminates the residual steady-state error.
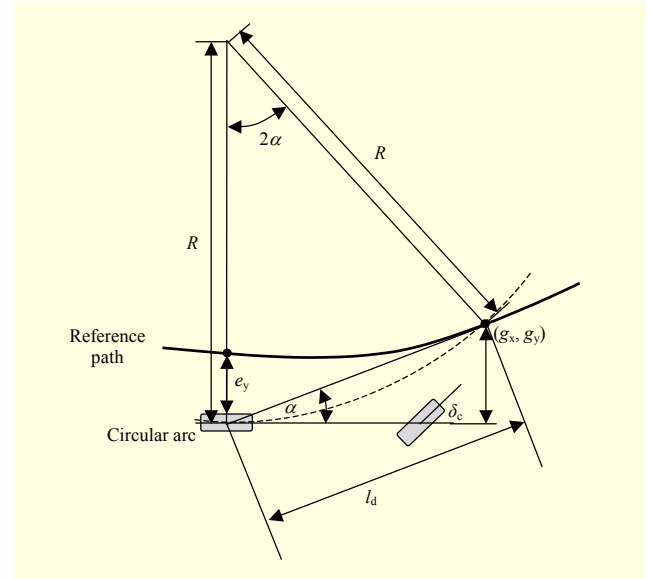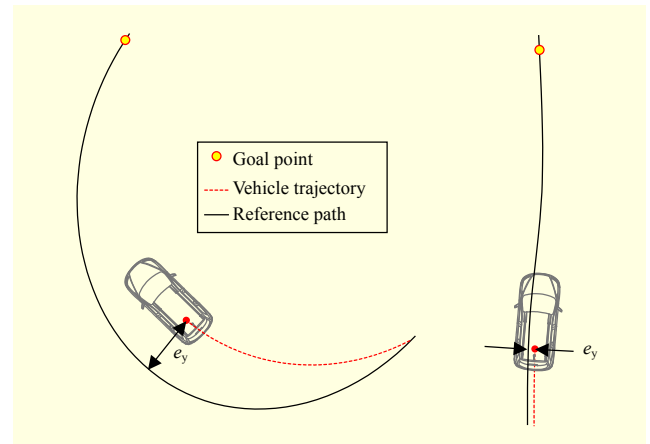

Fig. 8. Pure pursuit geometry.

Fig. 9. Examples of lateral offset (left: cutting corners and right: steady-state error).

$$\delta_{e_{\mathrm{y}}}(t) = \mathcal{P}e_{\mathrm{y}}(t) + \mathcal{Q}(\kappa(t))\int e_{\mathrm{y}}\mathrm{d}t. \tag{15}$$

The integral gain is a function of the road curvature.

The total desired steering angle, δ_{t}, is given through the following equation:

$$\delta_{\mathrm{t}} = \delta_{l_{\mathrm{d}}} + \delta_{e_{\mathrm{y}}}, \tag{16}$$

where $\delta_{l_{\mathrm{d}}}$ is the desired steering angle by look-ahead distance.

V. Primitive Driver

The primitive driver as a low-level controller drives the actuators to move the autonomous vehicle. The primitive driver consists of a throttle/brake controller and steering controller.

1. Steering Controller

The steering controller controls the steering actuator to follow the desired steering angle.

A. PID Controller

The advantages of a PID controller are its easy design and good performance. Thus, a PID controller has been used in many applications. Figure 10 shows a block diagram of the steering controller using a PID controller. The error, the difference between the desired steering angle and actual steering angle, is sent to the PID controller, and the controller computes the pulse-width modulation (PWM) signal. This signal is sent to the motor, and the steering motor controls the steering handle using the output torque. A mathematical description of a typical PID controller is shown in (17).

$$\text{MV}(t) = K_{\text{p}}e(t) + K_{\text{i}}\int_0^t e(\tau)\mathrm{d}\tau + K_{\text{d}}\frac{\mathrm{d}e}{\mathrm{d}t}, \tag{17}$$

where K_{p}, K_{i}, and K_{d} are the proportional gain, integral gain, and derivative gain, respectively, which we determine experimentally [11].

We verified the steering controller designed using a PID controller on a straight asphalt road. In this test, a longitudinal speed of 40 kph is used. Figure 11 shows the results. The red line in the figure is the desired steering angle, the black dotted line is the current steering angle, the green dotted line is the percent of torque value, and the blue line is the lateral offset.

Checking the actual steering angle data, we can see sections without a variation for a short period of time in spite of the motor torque output. In such sections, because the motor torque value is small, the movement of the steering handle is not influenced by the steering motor. This is called the dead band, and it occurs within a range of –6% to 6% torque. As a result, it generates a time delay of about 2 s when following the desired steering angle. In spite of the straight road and low speed, a lateral offset occurs at more than 0.3 m, and the more the vehicle velocity increases, the more the lateral error increases.

The reason for the dead band is the hardware characteristic of the steering system. Because the developed steering system transmits the torque using a toothed belt and pulley, some physical elements exist, such as a backlash, which interfere with the controls. To fix this problem, we designed a dead band
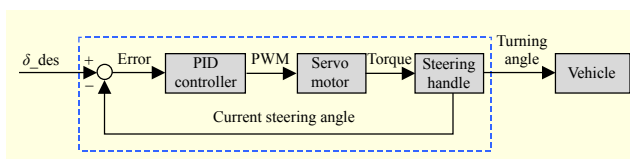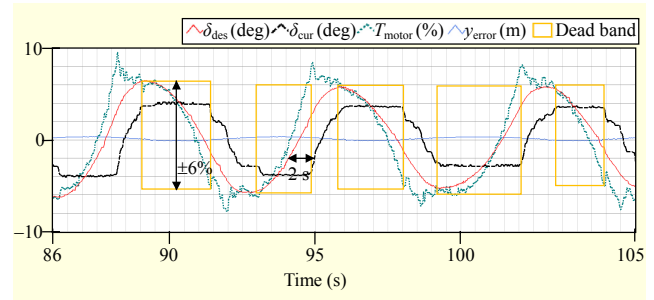

Fig. 11. Experimental results of steering controller using PID controller.
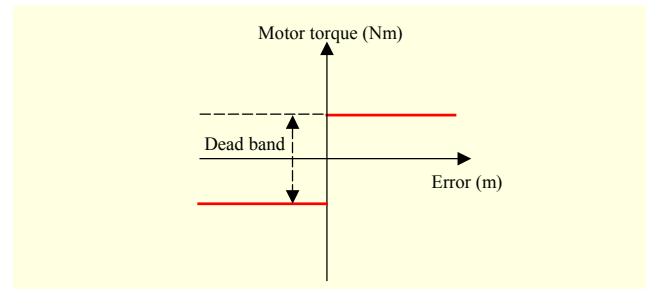

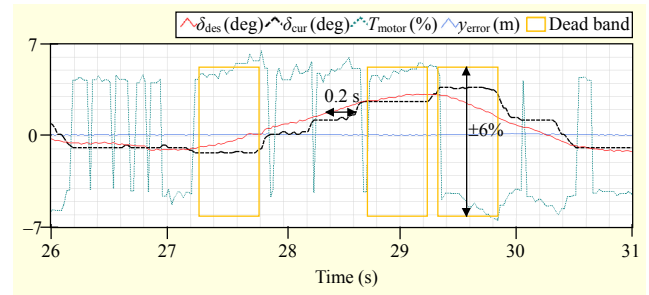Fig. 12. Dead band compensator.

Fig. 13. Experimental results of steering controller using PID controller and dead band compensator.
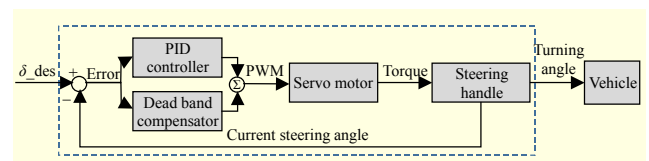

Fig. 14. Block diagram of steering controller using PID controller and dead band compensator.

compensator.

B. PID Controller and Dead Band Compensator

To reduce the time delay and lateral error, in this paper, we designed a dead band compensator (see Fig. 12). To immediately follow the desired angle, the dead band compensator compensates the minimum torque needed to

Fig. 10. Block diagram of steering controller using PID controller.

move the steering handle. The sign of the compensated torque depends on the sign of the error. If the error of the block diagram is positive, then the compensated torque is about 6%. If the error of the block diagram is negative, the compensated torque is about –6%, as shown in Fig. 13. The final desired output value is the sum of the output of each controller. Figure 14 shows a block diagram of the steering controller using a PID controller and dead band compensator.

We verified the steering controller designed using a PID controller and dead band compensator. In our test, a longitudinal speed of 80 kph is used. Figure 13 shows the results. As shown in the graph, the dead band section still exists, but the time delay decreases from 2 s to 0.2 s. In addition, the improving controller reduces the lateral error by about 0.24 m.

VI. Experimental Results

To verify the proposed steering control system, autonomous vehicles were tested on a typical asphalt road, as shown in Fig. 15. The distance of the test road is about 800 m, and the road has two lanes, where the width of each lane is 3.5 m in each direction. We conducted two different types of experiments to verify the steering control system. One is a lane following maneuver, and the other is a double change maneuver. In these tests, longitudinal speeds of 80 kph and 100 kph were used.

1. Lane Following Maneuver

The experimental environment consists of a straight section and curved section with a road curvature of 0.15. Figures 16 and 17 show the experimental results of the lane following maneuver.

Because of the influence of the dead band, the performance of the steering controller is not perfect, but the path tracking performance is good. The maximum lateral errors are about 0.24 m and 0.3 m in each longitudinal velocity in spite of the high velocity.

2. Double Lane Change Maneuver

The experimental environment for this maneuver consists of a straight section and curved section with a road curvature of 0.15.

The path of a double lane change maneuver is schematized in Fig. 18. The experimental environment in this maneuver consists of a straight section and a lane change section. For highways, the mean lane change durations range from 5.14 s to 6 s [12]–[13]. The lane change lengths are calculated to be between 114 m and 133 m at 80 kph, and between 138 m and
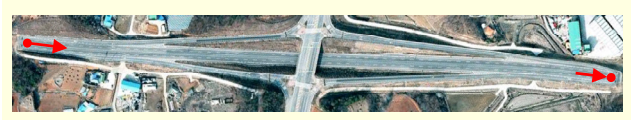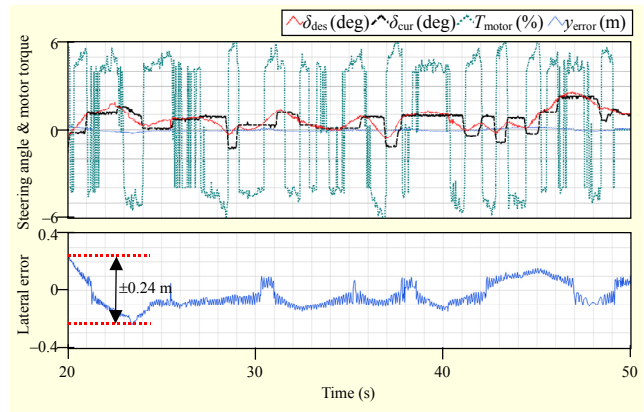

Fig. 15. Test road: typical asphalt road.

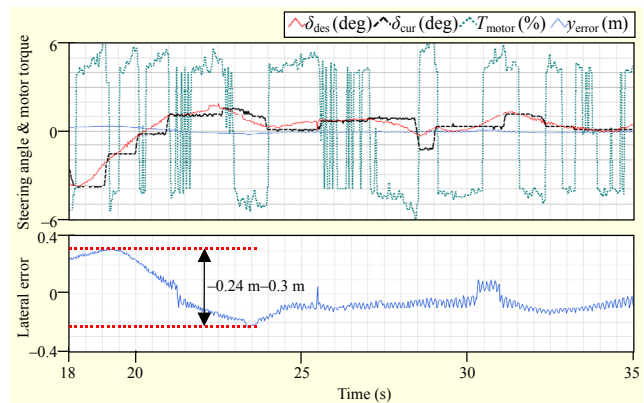Fig. 16. Experimental results of lane following maneuver at test velocity of 80 kph.

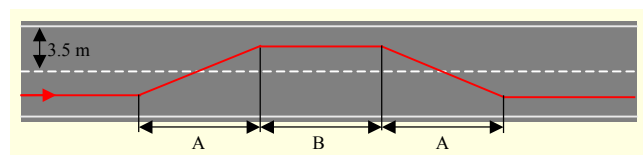Fig. 17. Experimental results of lane following maneuver at test velocity of 100 kph.

Fig. 18. Schematization of test road for double lane change maneuver.

166 m at 100 kph. Thus, during this maneuver, the lengths of lane change section A were set at 100 m and 150 m. In addition, the lengths of section B were set at 100 m and 150 m. Figures 19 and 20 show the experimental results of the double lane change maneuver using a path length of section A of 100 m. The performance of the steering controller is similar to
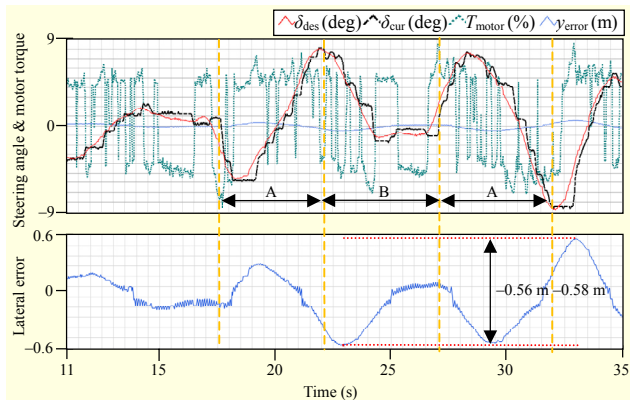
Fig. 19. Experimental results of double lane change for vehicle velocity of 80 kph and lane change section length of 100 m.
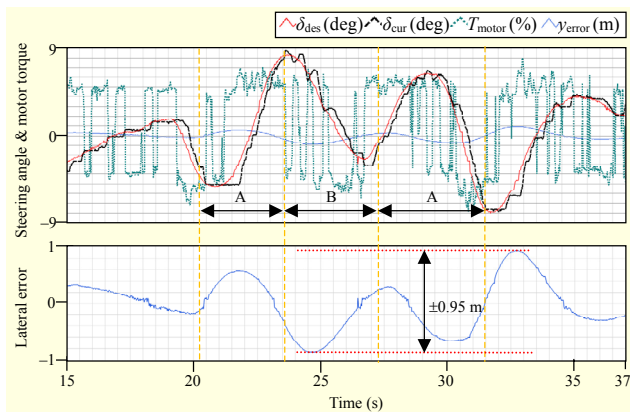

Fig. 20. Experimental results of double lane change for vehicle velocity of 100 kph and lane change section length of 100 m.
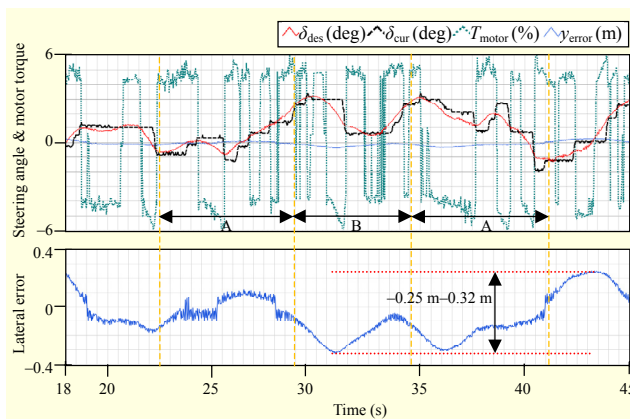

Fig. 21. Experimental results of double lane change for vehicle velocity of 80 kph and lane change section length of 150 m.

the results of the lane following maneuver. However, the overshoots occur immediately after the autonomous vehicle enters and exits the lane change section. In Fig. 19, the
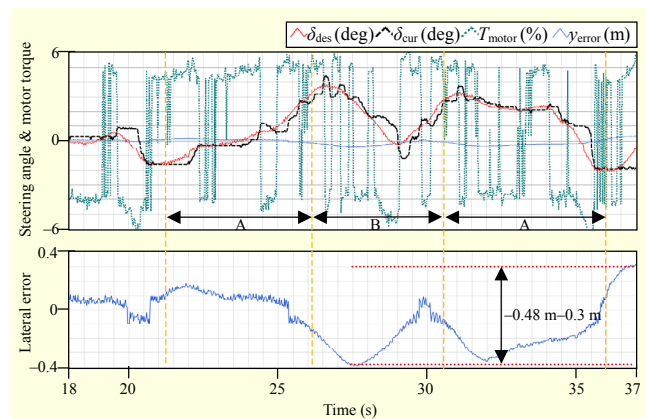

Fig. 22. Experimental results of double lane change for vehicle velocity of 100 kph with lane change section length of 150 m.

maximum lateral error is about 0.58 m at 80 kph. In Fig. 20, the maximum lateral error is about 1 m at 100 kph. As a result of a large lateral error, the vehicle departed the lane.

Figures 21 and 22 show the experimental results of a double lane change maneuver using a path length of of 150 m. The performance of the steering controller is similar to the results of other experiments. In addition, overshoots occurred. However, because the length of the lane change increased, the overshoot was reduced by 50%. The results show that the maximum lateral errors are about 0.32 m and 0.48 m at each velocity. As a result of the double lane change maneuver, if the lane change length increases, then the vehicle can stably change lanes.

VII. Conclusion

For this paper, we developed a steering control system for the path tracking of an autonomous vehicle. A servo motor was installed to control a steering handle, and it can transmit the steering force using a belt and pulley. The steering control system is a path tracking system that controls the steering actuator based on the current vehicle position, heading from the INS, and reference path from the path planner. The method for applying an autonomous vehicle to path tracking is an advanced pure pursuit method that can reduce cutting corners, which is a weakness of the pure pursuit method.

We designed the steering controller to apply to a PID controller using an error; that is, the difference between the desired steering angle and actual steering angle. However, because of some physical elements, the dead band is a finite range in which the system cannot detect the output variation. Based on the influence of the dead band, the performance of the path tracking and stability of the autonomous vehicle are reduced. We developed a dead band compensator to overcome a dead band, and improved the path tracking performance and

stability.

Two different kinds of experiments were conducted to verify the steering control system. In the lane following maneuver, the lateral error was 0.3 m or less in spite of a high velocity. In a double lane change maneuver, an overshoot occurred for a short lane change length. When the lane change length increases, stable driving of the vehicle is possible.

In this paper, we assumed that there is no influence on the disturbances (crosswind, driver torque) and did not apply tire or road models. For this reason, the lateral errors do not converge near to zero.

In our future work, to reduce the tracking error, we need to develop a model-based algorithm that is independent of the curvature of the road. In addition, more experiments are required to verify the system under various environments.

References

[1] O. Tunçer et al., "Vision Based Lane Keeping Assistance Control Triggered by a Driver Inattention Monitor," *IEEE Int. Conf. Syst., Man, Cybern.*, Istanbul, Turkey, Oct. 10–13, 2010, pp. 289–297.

[2] Y. Wang and X. Zhu, "Design and Implementation of an Integrated Multi-functional Autonomous Parking System with Fuzzy Logic Controller," *American Cont. Conf.*, Montreal, Canada, June 27–29, 2012, pp. 2928–2933.

[3] J.M. Snider, "*Automatic Steering Methods for Autonomous Automobile Path Tracking*," M.S. thesis, Robot. Institute, Carnegie Mellon Univ., Pittsburgh, PA, USA, Feb. 2009.

[4] J.S. Wit, "*Vector Pursuit Path Tracking for Autonomous Ground Vehicles*," Ph.D. dissertation, Dept. Mechanical and Aerospace Eng., Univ. of Florida, Gainesville, USA, 2000.

[5] A. Sugiyama et al., "An EPS Control Strategy to Reduce Steering Vibration Associated with Disturbance from Road Wheels," *SAE World Congress Exhibition*, Detroit, MI, USA, 2006.

[6] S.Y. Cho and H.K. Lee, "Modified RHKF Filter for Improved DR/GPS Navigation against Uncertain Model Dynamics," *ETRI J.*, vol. 34, no. 3, June 2012, pp. 379–387.

[7] M. Enkhtur, S.Y. Cho, and K.-H. Kim, "Modified Unscented Kalman Filter for a Multirate INS/GPS Integrated Navigation System," *ETRI J.*, vol. 35, no. 5, Oct. 2013, pp. 943–946.

[8] B. Park and W.Y. Han, "Reference Velocity Estimation Method for O-Rad Unmanned Ground Vehicle," *Int. Conf. Ubiquitous Robots Ambient Intell.*, Jeju, Rep. of Korea, Oct. 30–Nov. 2, 2013, pp. 230–231.

[9] C. Chen and H.-S. Tan, "Experimental Study of Dynamic Look-ahead Scheme for Vehicle Steering Control," *American Contr. Conf.*, San Diego, CA, USA, June 2–4, 1999, pp. 3163–3167.

[10] S.F. Campbell, "*Steering Control of an Autonomous Ground Vehicle with Application to the DARPAR Urban Challenge*," M.S. thesis, Dept. Mechanical Eng., Massachusetts Institute of Technology, Cambridge, USA, 2007.

[11] K.H. Ang, G. Chong, and Y. Li, "PID Control System Analysis, Design, and Technology," *IEEE Trans. Contr. Syst. Technol.*, vol. 13, no. 4, July 2005, pp. 559–576.

[12] J.E. Naranjo et al., "Lane-Change Fuzzy Control in Autonomous Vehicles for the Overtaking Maneuver," *IEEE Trans. Intell. Transp. Syst.*, vol. 9, no. 3, Sept. 2008, pp. 438–450.

[13] L.-S. Jin et al., "Research on Safety Lane Change Model of Driver Assistant System on Highway," *IEEE Intell. Vehicles Symp.*, Xi'an, China, June 3–5, 2009, pp. 1051–1056.

Myungwook Park received his BS degree in mechanical engineering from the Engineering College, Kookmin University, Seoul, Rep. of Korea, in 2006 and his MS and PhD degrees in electronic control systems from the School of Automotive Engineering, Kookmin University, in 2008 and 2012, respectively. Since 2013, he has been with the Electronics and Telecommunications Research Institute, Daejeon, Rep. of Korea, where he is now a senior researcher. His main research interests are autonomous vehicles, vehicle electronic control systems, and control theory.

Sangwoo Lee received his BS and MS degrees in electronic communication engineering from the Engineering College, Kwangwoon University, Seoul, Rep. of Korea, in 1994 and 1996, respectively. From 1996 to 2000, he worked for Daewoo Electronics, Seoul, Rep. of Korea. Since 2000, he has been with the Electronics and Telecommunications Research Institute, Daejeon, Rep. of Korea, where he is now a principal researcher. His main research interests are vehicular communication, intelligent transportation systems, and autonomous driving systems.

Wooyong Han received his BS and MS degrees in electronics engineering from the Engineering College, Kyung Hee University, Yongin, Rep. of Korea, in 1983 and 1985 and his PhD degree in computer science from the Department of Computer Science and Engineering, Chungnam National University, Daejeon, Rep. of Korea, in 2005. Since 1989, he has been with the Electronics and Telecommunications Research Institute, Daejeon, Rep. of Korea, where he is now a principal researcher. His main research interests are object-oriented distributed computing; XML-based e-commerce common frameworks; XML-based B2B system interoperability; XML digital signature and encryption; frameworks for telematics applications independent of mobile networks; vehicles; and territorial digital multimedia broadcasting.